Agricultural and Forest Meteorology 275 (2019) 233–242

Contents lists available at ScienceDirect

Agricultural and Forest Meteorology

journal homepage: www.elsevier.com/locate/agrformet

# Impacts of diffuse radiation fraction on light use efficiency and gross primary production of winter wheat in the North China Plain

Xiaoya Yang[a,*], Jun Li[b], Qiang Yu[c,d], Yuchun Ma[a], Xiaojuan Tong[e], Yan Feng[f,g], Yingxiang Tong[g]

[a] Jiangsu Key Laboratory of Agricultural Meteorology, College of Applied Meteorology, Nanjing University of Information Science and Technology, Nanjing, 210044, China
[b] Key Laboratory of Water Cycle & Related Land Surface Processes, Institute of Geographic Sciences and Natural Resources Research, Chinese Academy of Sciences, Beijing, 100101, China
[c] State Key Laboratory of Soil Erosion and Dryland Farming on the Loess Plateau, Northwest A&F University, Yangling, 712100, China
[d] School of Life Sciences, University of Technology Sydney, PO Box 123, Broadway, NSW, 2007, Australia
[e] College of Forestry, Beijing Forestry University, Beijing, 100101, China
[f] Key Laboratory of Atmospheric Science and Satellite Remote Sensing, Anhui Institute of Meteorology, Hefei, 230031, China
[g] Shouxian National Climate Observatory, Shouxian, 232200, China

ARTICLE INFO

*Keywords:*
Light use efficiency
Gross primary production
Diffuse radiation fraction
Radiation partitioning model
Winter wheat

ABSTRACT

The increase of diffuse radiation fraction ($k_d$) has been reported to significantly impact light use efficiency (LUE) and carbon uptake in terrestrial ecosystems. The impact of $k_d$ on LUE should be considered in crop models to accurately evaluate the effect of radiation changes on crop production. However, the magnitude of the $k_d$ effect is difficult to quantify because of the complicated interacting relationships among all of the meteorological parameters, as well as the changing effects for various ecosystem types and research sites. Eight site-years of flux data and two years of diffuse radiation data from two field ecosystems in the North China Plain were used to (1) compare the performance of five $k_d$ models, (2) explore the impacts of environmental factors on LUE and gross primary production (GPP) of winter wheat (*Triticum aestivum* L.), and (3) quantify the relationships between $k_d$ and both LUE and GPP of winter wheat. Comparison results showed that the $k_d$ model developed by Boland et al. performed the best of the five models evaluated. This model was chosen to calculate $k_d$ in this research. Path analysis show that $k_d$ was the main factor affecting LUE of winter wheat, explaining up to 55% of the variability in LUE. The relationship between $k_d$ and LUE was significantly linear (slope of about 0.326 g C $mol^{-1}$). GPP initially increased and then decreased with increasing $k_d$. A moderate radiation condition ($k_d$ = 0.53) was favorable for increasing GPP. The effect of $k_d$ on LUE should be added in the LUE module of APSIM-Nwheat to improve simulation accuracy. The results of this study highlight the importance of $k_d$ in correctly modeling LUE for winter wheat with a crop model and provide quantitative relationships between these two parameters. These relationships will be helpful in improving crop model simulation accuracy under changed climate conditions.

## 1. Introduction

The increase of clouds and aerosols in China has reduced total solar radiation reaching the earth's surface, resulting in an increase in $k_d$, the ratio between diffuse radiation and total solar radiation (Schiermeier, 2006; Ren et al., 2013). Both observations and modeling studies have reported that the increase in $k_d$ improved LUE of the plant (Gu et al., 2002; Dengel and Grace, 2010; Oliphant et al., 2011). The mechanism of this phenomenon was that highly diffuse conditions reduced the light saturation limit for upper canopy leaves and better illuminated the lower canopy (Gu et al., 2002; Greenwald et al., 2006; Williams et al., 2016).

The importance of including the effect of $k_d$ on LUE in the simulation of ecosystem productivity has been recommended in previous studies (e.g. Zhang et al., 2011; Wang et al., 2015; Wang et al., 2018). Yuan et al. (2014) found that six LUE or GPP models significantly underestimated GPP during cloudy days when $k_d$ was not considered. Changes in $k_d$ not only affect LUE and GPP of ecosystems, but also have important effects on crop yield. The LUE modules used in cropping systems models need to add the effect of $k_d$ to accurately simulate the influence of diffuse radiation changes on crop production (Greenwald et al., 2006; Chen et al., 2010). The linear relationships between $k_d$ and LUE of winter wheat and maize were added to the APSIM crop model (Chen et al., 2010) according to the research results of Choudhury

* Corresponding author.
*E-mail address:* yangxy@nuist.edu.cn (X. Yang).

https://doi.org/10.1016/j.agrformet.2019.05.028
Received 10 October 2018; Received in revised form 24 May 2019; Accepted 28 May 2019

(2000, 2001) and Rodriguez and Sadras (2007). Greenwald et al. (2006) found that changes in crop yield due to the influence of aerosols were greatly dependent on the magnitude of the increase in LUE resulting from increasing $k_d$. Alton et al. (2007) reported that the enhancement of diffuse radiation on LUE varied greatly among different research results. Quantitative analysis of the impact of $k_d$ on crop LUE is important to accurately evaluate the effect of changed total and diffuse radiation on crop production. Observations of 30-min $CO_2$ flux by an eddy covariance system in the field provide the possibility of analyzing the quantitative relationship between $k_d$ and LUE on a daily time scale. Such results would provide the scientific basis for improving LUE modules used in crop models.

Diffuse radiation has not been observed at many experimental sites, or has only been observed in recent years. Many studies have estimated $k_d$ using radiation partitioning models (Gu et al., 2002; Lee et al., 2018). These models originated from the research of Liu and Jordan (1960), who estimated $k_d$ in terms of the sky clearness index ($k_t$). Quite a few similar models were developed later (e.g. Erbs et al., 1982; Spitters et al., 1986; Reindl et al., 1990; Boland et al., 2008), each of which successfully fit $k_d$ data within a specified region. Comparisons among these $k_d$ models were made by using different datasets (Dervishi and Mahdavi, 2012; Kuo et al., 2014) to evaluate the performance of these models. The comparison results varied with site due to differences in geographic or climatic factors such as cloud cover and type and particulate matter in the air (Cruse et al., 2015).

Variability in GPP observed by an eddy covariance system was attributed to the complex interaction of various biophysical factors, such as climate variables (temperature, solar radiation, and water vapor pressure), soil conditions, biotic factors, management, and application of pesticides/herbicides (Dunn et al., 2007; Wu et al., 2016). Among these biophysical factors, $k_d$ has been noted to have a significant influence on GPP (Gu et al., 2003; Kanniah et al., 2012). The response of GPP to the increase in $k_d$ depends on plant species, canopy structure, leaf area index (LAI), and growth environment (Kanniah et al., 2012; Cheng et al., 2015). Enhanced LUE due to increased $k_d$ would increase GPP, while the decrease of PAR induced by an increase in $k_d$ would reduce GPP. The final impact of these two opposing effects on GPP of different ecosystems remains to be clarified, especially on the basis of observational data. Research on the comprehensive effects of $k_d$ and PAR on GPP are important for assessing the impacts of climate change on ecosystem productivity (Jing et al., 2010; Kanniah et al., 2013).

The North China Plain is the primary winter wheat production region in China (Yang et al., 2018). The atmospheric aerosols of this region have increased in recent years due to increasing population and industrial development (Yang et al., 2016). Research on the impact of $k_d$ on LUE and GPP of wheat based on field observations has been helpful in estimating climate change effects on wheat production in the North China Plain. The objectives of this research were to (1) compare the performance of different $k_d$ models in the North China Plain, (2) explore the impacts of environmental factors on LUE and GPP of winter wheat, and (3) quantify the relationships between $k_d$ and both LUE and GPP of winter wheat in the North China Plain.

## 2. Materials and methods

### 2.1. Site descriptions

Field observations were conducted at Yucheng Comprehensive Experiment Station (YC) and Shouxian National Climate Observatory (SX), which are located in the northern and southern regions of the North China Plain, respectively. The YC has a semiarid and warm temperate monsoon climate. The SX is located on the south bank of the middle reaches of the Huaihe River, with a sub-humid and subtropical monsoon climate. The SX site is warmer and wetter than YC. The annual mean precipitation of SX is nearly double that of YC (Table 1). The typical cropping systems are two-year rotations, with winter wheat and summer maize (*Zea mays* L.) at YC, and winter wheat and rice (*Oryza sativa* L.) at SX. Detailed descriptions of the two sites are provided in Table 1. Winter wheat was planted in mid/late October and harvested in late May or early June at these two experimental sites. The maximum height of winter wheat was 89 cm at YC and 81 cm at SX.

**Table 1**
Site descriptions.

| Site | Yucheng (YC) | Shouxian (SX) |
|---|---|---|
| Location | 36°57′N, 116°38′E | 32°30′N, 116°46′E |
| Elevation (m) | 23.4 | 22.7 |
| Annual mean temperature (°C) | 13.1 | 15.0 |
| Annual mean precipitation (mm) | 528 | 1022 |
| Typical cropping system | Winter wheat and summer maize rotation | Winter wheat and rice rotation |
| Soil type | Tidal soil | Tidal soil |
| Soil texture | Sandy loam | Clay |
| The maximum height of wheat (cm) | 89 | 81 |
| OPEC height (m)[a] | 2 | 4 |
| Radiometer height (m)[a] | 2 | 4 |
| Air temperature and humidity profile measurement heights (m)[a] | 2, 3 | 2, 4, 10, 20, 30 |
| Soil temperature depths (cm)[a] | 2, 5, 20, 50, 100 | 5, 10, 15, 20, 40 |
| Soil moisture depths (cm)[a] | 20, 40 | 10, 20, 50, 100, 180 |

OPEC, open path eddy covariance instrumentation.
[a] Height of the sensors mounted at the location.

### 2.2. Field observations

$CO_2$ and latent heat fluxes were measured with an eddy covariance system with an open path $CO_2/H_2O$ gas analyzer (model LI-7500, Li-Cor Inc., Nebraska, USA) and a 3-D sonic anemometer (model CSAT3, Campbell Sci. Inc., Utah, USA). The signals of the instruments were recorded at 10 Hz by a model CR5000 datalogger at YC and by a model CR1000 datalogger at SX (both dataloggers manufactured by Campbell Scientific Inc., Utah, USA). The open-path eddy covariance (OPEC) system was installed at the height of 2 m at YC and at a height of 4 m at SX (Table 1). The upwind fetch distances were more than 200 m and 400 m at YC and SX respectively.

Routine meteorological variables were measured simultaneously with the fluxes determined by eddy covariance at each of the sites. Air temperature, humidity, and water vapor pressure were measured with shielded and aspirated probes (model HMP45C, Vaisala, Finland). The observations of air temperature and humidity at 2 m were used in this research. PAR was measured using a quantum sensor (model LI-190SB, Li-Cor Inc, Nebraska, USA). Solar radiation was measured with a pyranometer (model CM11, Kipp & Zonen, Delft, The Netherlands). Rainfall was measured with a rain gauge (model 52203, R.M Young, Michigan, USA). All meteorological measurements were recorded at 30-min intervals with data loggers (model CR23x, Campbell Sci. Inc., Utah, USA). Soil temperature was monitored using thermocouple probes (model 105E, Campbell Scientific Inc., Utah, USA). Soil water content (SWC) was measured with time domain reflectometers (model CS616, Campbell Sci. Inc., Utah, USA). The SWC measurements at depths of 20 and 40 cm at YC and 10, 20, and 50 cm at SX were averaged to provide daily SWC values over the growing season. Daily average air temperature (Ta) was computed from the 30-min values each day. Daily vapor pressure deficit (VPD) was computed from the daytime 30-min values each day.

Hourly total and diffuse radiation on the horizontal plane from 2015 to 2016 at SX were measured by pyranometers (model CMP22, Kipp & Zonen, Delft, The Netherlands). The height of the pyranometers was 2 m above the soil surface. Daily total and diffuse radiation were calculated on the basis of this dataset, and 708 daily data points were

**Table 2**
Cultivar, sowing date, plant density, and irrigation times for each growing season at Yucheng (YC) and Shouxian (SX), China.

| Station | Year | Cultivar | Sowing date | Plant density (pl $m^{-2}$) | Irrigation times |
|---|---|---|---|---|---|
| YC | 2003–2004 | Keyu 13 | 23 Oct 2003 | 220 | overwintering, jointing, and flowering stages |
| | 2004–2005 | Keyu 13 | 18 Oct 2004 | 220 | overwintering, jointing, and flowering stages |
| | 2005–2006 | Keyu 13 | 19 Oct 2005 | 220 | overwintering, returning green, and flowering stages |
| | 2007–2008 | Kenong 199 | 25 Oct 2007 | 240 | overwintering and returning green |
| SX | 2007–2008 | Wanmai 53 | 22 Oct 2007 | 230 | not irrigated |
| | 2008–2009 | Yumai 70-36 | 16 Oct 2008 | 250 | not irrigated |
| | 2009–2010 | Wanmai 50 | 18 Oct 2009 | 230 | not irrigate |
| | 2010–2011 | Jinfeng 3 | 24 Oct 2010 | 250 | not irrigated |

obtained after deleting days with missing data.

Measurements were made during winter wheat growing seasons from 2004 to 2006 and 2008 at YC, and from 2008 to 2011 at SX. These years were selected for this analysis due to better data quality. The cultivar and sowing date of each growth season are listed in Table 2. Plant density was observed at the three-leaf stage. Winter wheat was irrigated two or three times (at the overwintering, returning green or jointing, and flowering stages) by flooding. Fertilizer was applied twice (before sowing and at jointing stage) at YC. Winter wheat was fertilized once (before sowing) at SX. The amounts of nitrogen (N) fertilizer application were about 220 and 230 kg N $ha^{-1}$ during each wheat season at YC and SX, respectively. There was no irrigation at SX due to the greater precipitation and high groundwater table at the location which on average provided enough available water during wheat growing seasons to minimize water stress conditions. Chemical weed control was used at both locations. No serious pest and disease problems occurred during any of the growing seasons. Leaf area index was measured at several growth stages with a leaf area meter (model LI-3100, Li-Cor, Inc., Nebraska, USA) at YC. There were no LAI measurements taken at SX. In each of the four years of the study, wheat LAI showed a typical development pattern, increasing to a maximum and then decreasing with time (Fig. 1). Therefore, in order to exclude the effect of LAI changes on the net ecosystem exchange of $CO_2$ (NEE) and corresponding meteorological data, only data from jointing to milky maturity growth stages (when canopy cover was at or near full cover, LAI > 3), were chosen for this study. The specific dates of each year's study period are shown in Table 3 and Fig. 1.

### 2.3. Data processing

#### 2.3.1. Flux data processing

Raw $CO_2$ flux data were processed by two-dimension coordinate rotations (McMillen, 1988) and Webb-Pearman-Leuning (WPL) correction (Webb et al., 1980) to obtain 30-min mean flux data. The coordinate rotations were applied to force the average vertical wind speed to zero. WPL correction was used to correct flux data according the variation of air density caused by transfer of heat and water vapor. $CO_2$ flux data affected by rain and dew were eliminated following the method used by Falge et al. (2001). The nighttime data were deleted when friction velocity was lower than 0.15 m $s^{-1}$ (Li et al., 2006; Tong et al., 2017), as $CO_2$ flux would be misestimated due to weak turbulence. Negative $CO_2$ flux values during nighttime were removed because there was no photosynthesis during nighttime (Zhu et al., 2006). Data gaps were filled by using mean diurnal variation (MDV) (Falge et al., 2001; Yu et al., 2008).

The ratios of missing and excluded data to the total data volume are shown in Table 4. The percentages of the total missing data ranged between 21.0 and 34.3% for different growing seasons. On average, only 3.8% of daytime data were missing. Most of the missing data was from nighttime hours. The daily GPP data were used in this research. If the missing half hourly daytime data in one day accounted for more than 25% of total daytime data, then this day was deleted from data volume. The number of days which were deleted from each research period (from jointing to milky maturity) are shown in Table 4. The number of deleted days ranged between two and seven days. There was rain on almost all of these deleted days.

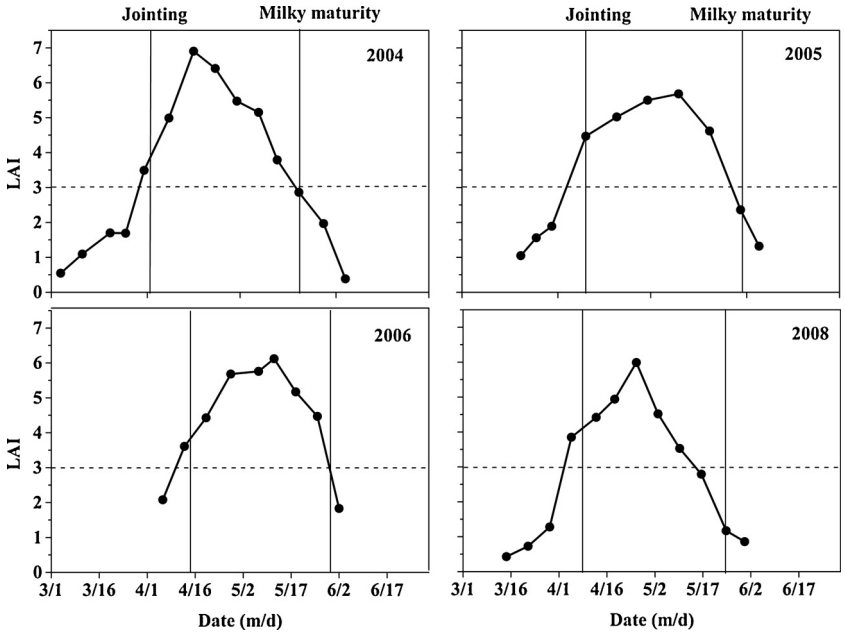


**Fig. 1.** Leaf area index (LAI) of winter wheat from 2004 to 2006 and 2008 at Yucheng, China.

**Table 3**
Environmental conditions from jointing to milky maturity of winter wheat at Yucheng (YC) and Shouxian (SX), China.

| Station | Year | Jointing | Milky maturity | PAR (mol $m^{-2}$ $d^{-1}$) | Temperature (°C) | VPD (hPa) | Precipitation (mm) | SWC ($m^3$ $m^{-3}$) |
|---|---|---|---|---|---|---|---|---|
| YC | 2004 | 2 Apr. | 20 May | 26.2 | 16.6 | 9.1 | 55 | 0.35 |
| | 2005 | 10 Apr. | 31 May | 31.5 | 17.8 | 10.2 | 33 | 0.45 |
| | 2006 | 14 Apr. | 31 May | 29.7 | 17.6 | 9.1 | 84 | 0.39 |
| | 2008 | 7 Apr. | 25 May | 27.1 | 17.1 | 8.8 | 95 | 0.51 |
| SX | 2008 | 17 Mar. | 15 May | 31.6 | 15.7 | 7.1 | 193 | 0.59 |
| | 2009 | 7 Mar. | 9 May | 30.7 | 14.6 | 7.5 | 104 | 0.57 |
| | 2010 | 15 Mar. | 14 May | 27.2 | 13.9 | 6.5 | 196 | 0.61 |
| | 2011 | 20 Mar. | 17 May | 34.0 | 17.2 | 11.6 | 60 | 0.49 |

PAR, photosynthetically active radiation; VPD, vapor pressure deficit; SWC, soil water content.

**Table 4**
The ratios for number of missing $CO_2$ flux data to total data volume during the research period at Yucheng (YC) and Shouxian (SX) (%). Number of days from jointing to milky maturity in each growing season, and the deleted number of days are also listed.

| Station | Year | Total | Nighttime | Daytime | Number of days | Deleted number of days |
|---|---|---|---|---|---|---|
| YC | 2004 | 28.6 | 24.4 | 4.2 | 49 | 4 |
| | 2005 | 31.4 | 28.7 | 2.7 | 52 | 4 |
| | 2006 | 21.0 | 18.3 | 2.7 | 48 | 3 |
| | 2008 | 30.5 | 26.6 | 3.9 | 49 | 3 |
| SX | 2008 | 29.7 | 26.6 | 3.1 | 60 | 5 |
| | 2009 | 34.3 | 29.7 | 4.6 | 64 | 3 |
| | 2010 | 31.1 | 25.0 | 6.1 | 61 | 7 |
| | 2011 | 32.2 | 29.5 | 2.7 | 59 | 2 |

#### 2.3.2. Gross primary production

GPP was calculated as:

$$GPP = R_e - NEE \quad (1)$$

NEE was obtained directly from the eddy covariance measurement ($CO_2$ flux data). Daytime ecosystem respiration ($R_e$) was estimated using the equation given in Lloyd and Taylor (1994):

$$R_e = R_{ref}\, e^{E_0\left(\frac{1}{T_{ref}-T_0}-\frac{1}{T_s-T_0}\right)} \quad (2)$$

where $T_s$ is soil temperature (°C) at 5 cm soil depth. $T_0$ is a constant, set at -46.02 °C, $E_0$ is a parameter that essentially determines the temperature sensitivity of ecosystem respiration, $R_{ref}$ represents the ecosystem respiration rate at a reference temperature ($T_{ref}$, 10 °C). The nighttime NEE values, which also are the night ecosystem respiration ($R_e$) under turbulent conditions, were used to estimate $R_{ref}$ and $E_0$ in Eq. (2). Then the estimated $R_{ref}$ and $E_0$ were used to calculate daytime ecosystem respiration. Daytime $R_e$ may be overestimated because negative nighttime NEE values were removed. This may have resulted in an overestimation for GPP.

Daily GPP (g C $m^{-2}$ $d^{-1}$) was obtained by summing the daytime 30-min GPP values (mg $CO_2$ $m^{-2}$ $s^{-1}$) and then multiplying by 1.8 × 12/44 (unit conversion coefficient). Daytime is defined as when the solar elevation angle is greater than 0°.

#### 2.3.3. Ecosystem light use efficiency

Daily LUE (g C $mol^{-1}$) was defined as the ratio of daily GPP (g C $m^{-2}$ $d^{-1}$) to incident daily PAR (mol $m^{-2}$ $d^{-1}$),

$$LUE = \frac{GPP}{PAR} \quad (3)$$

Daily PAR was obtained by summing daytime 30-min PAR values (μmol $m^{-2}$ $s^{-1}$) and then multiplying by 0.0018 (unit conversion coefficient).

### 2.4. Diffuse radiation fraction models

There were no observations of $k_d$ during our study at either research station. However, daily measured $k_d$ from 2015 to 2016 at SX were available and used for choosing the best performing model from five $k_d$ models. Three models (from Erbs et al. (1982), Spitters et al. (1986), and Zhou et al. (2004)) produced values of daily $k_d$, while the other two models (from Reindl et al. (1990) and Boland et al. (2008)) produced values of hourly $k_d$. The daily and hourly models have often had mixed use in previous studies (Ren et al., 2013; Kuo et al., 2014). The first author's surname is used to represent each model throughout the remainder of this paper. Based on the results of a comparative study of $k_d$ models (Dervishi and Mahdavi, 2012; Kuo et al., 2014), the better performing models (Erbs, Reindl and Boland) were chosen for this study. The model from Zhou et al. (2004) derived daily $k_d$ based on measured global and diffuse radiation data from 78 meteorological stations in China, so it was also chosen. Specific calculation equations for each model are listed in Table 5.

The five models simulated $k_d$ by using $k_t$. The $k_t$ is defined as the ratio of global solar radiation ($S_0$, MJ $m^{-2}$ $d^{-1}$) received at the Earth's surface to the extraterrestrial irradiance at a plane parallel to the Earth's surface ($S_e$, MJ $m^{-2}$ $d^{-1}$) (Gu et al., 1999):

$$k_t = \frac{S_0}{S_e} \quad (4)$$

The calculation of $S_e$ was according to FAO-56 (Allen et al., 2006). Three common statistical indicators were used to compare the

**Table 5**
Summary of the diffuse fraction models from the literature.

| | Constraints | | Diffuse fraction ($k_d$) |
|---|---|---|---|
| Erbs et al. (1982) | $w_s < 1.4208$ | $k_t < 0.715$ | $1.0 - 0.2727k_t + 2.4495k_t^2 - 11.9514k_t^3 + 9.3879k_t^4$ |
| | | $k_t \geq 0.715$ | 0.143 |
| | $w_s \geq 1.4208$ | $k_t < 0.722$ | $1.0 + 0.2832k_t - 2.5557k_t^2 + 0.8448k_t^3$ |
| | | $k_t \geq 0.722$ | 0.175 |
| Spitters et al. (1986) | $k_t < 0.07$ | | 1 |
| | $0.07 \leq k_t < 0.35$ | | $1 - 2.3(k_t - 0.07)^2$ |
| | $0.35 \leq k_t < 0.75$ | | $1.33 - 1.46k_t$ |
| | $k_t \geq 0.75$ | | 0.23 |
| Zhou et al. (2004) | $k_t < 0.2$ | | 0.987 |
| | $0.2 \leq k_t < 0.75$ | | $1.292 - 1.447k_t$ |
| | $k_t \geq 0.75$ | | 0.209 |
| Reindl et al. (1990) | $0 \leq k_t \leq 0.3$ | | $1.020 - 0.248k_t$ |
| | $0.3 < k_t < 0.78$ | | $1.45 - 1.67k_t$ |
| | $k_t \geq 0.78$ | | 0.147 |
| Boland et al. (2008) | None | | $1 / [1 + \exp(8.60k_t - 5.00)]$ |

$w_s$ was sunset hour angle, which can be calculated according to FAO-56 (Allen et al., 2006).

performance of the models: the relative error (RE), the relative mean bias deviation (MBD), and the root mean square deviation (RMSD) respectively. The three indicators were calculated as:

$$RE_i = \frac{k_{dm(i)} - k_{de(i)}}{k_{dm(i)}} \times 100\,(\%) \quad (5)$$

$$MBD = \frac{\sum_{i=1}^{n} \left(\frac{k_{dm(i)} - k_{de(i)}}{k_{dm(i)}}\right)}{n} \times 100\,(\%) \quad (6)$$

$$RMSD = \sqrt{\frac{\sum_{i=1}^{n} [(k_{dm(i)} - k_{de(i)})/k_{dm(i)}]^2}{n}} \quad (7)$$

In these equations, $k_{dm(i)}$ denotes the measured diffuse fraction, $k_{de(i)}$ denotes the estimated diffuse fraction, and n is the total number of pairs of measured and estimated values. Small absolute values of the MBD and the RMSD characterize better model performance.

### 2.5. LUE module in APSIM-Nwheat

The Agricultural Production Systems Simulator (APSIM) for wheat (APSIM-Nwheat version 1.55 s) is a crop simulation model (Keating et al., 2001). APSIM-Nwheat calculates potential daily biomass production based on light interception and LUE. Sub-optimal temperatures, water, and N-deficit can reduce the potential growth (Yang et al., 2013). More details about this crop model can be found in Asseng et al. (1998). In this model, daily LUE (g dry matter produced $MJ^{-1}$ $S_0$) is simulated using daily $S_0$:

$$LUE = \frac{3.8 \times S_0^{0.6}}{S_0} \quad (8)$$

This function considers an increasing LUE with decreasing $S_0$, following the CERES Wheat model approach (Ritchie et al., 1985), based on the results of wheat experiments (Spiertz and Van de Haar, 1978). The units of the calculated LUE can be converted to g C $mol^{-1}$ (PAR) assuming the carbon content of the dry matter to be 41% (van den Boogaard et al., 1996), and 1 MJ (PAR) to be equal to 4.6 mol photons (Wall and Kanemasu, 1990). PAR accounted for 33.1 and 39.6% of $S_0$ at YC and SX, respectively. Simulated LUE by this function is based on dry matter, which could be converted to GPP by dividing by the conversion factor of 0.61 (Watanabe, 1975).

### 2.6. Path analysis

Path analysis was used to qualitatively explore the impact of biophysical factors on GPP and LUE, as biophysical variables are usually highly correlated. Path analysis is a multiple regression technique that considers the covariance among variables. This method has been used to evaluate the impact of environment factors on carbon exchange in various ecosystems (Huxman et al., 2003; Wu et al., 2016; Wang et al., 2018). In this current study, path analysis was performed to partition the correlation coefficient, $r_{iy}$, into direct and indirect effects among variables. The direct effect value is the standardized partial regression coefficient, which means that independent variable i directly affects dependent variable y. The indirect effect represents how variable i influences another variable, j, which in turn affects the dependent variable, y.

$$r_{iy} = r_{i1}P_{1y} + r_{i2}P_{2y} + \ldots + r_{ii}P_{iy} + \ldots + r_{in}P_{ny}\ (i = 1, 2, 3, \ldots, n) \quad (9)$$

where $r_{iy}$ is the correlation coefficient between independent variable i and dependent variable y, $r_{in}$ is the correlation coefficient between variable i and variable n, $P_{iy}$ is the direct effect of independent variable i on dependent variable y, $r_{in}$ x $P_{ny}$ ($i \neq n$) is the indirect effect of variable i influencing another variable n which in turn affects the dependent variable y.

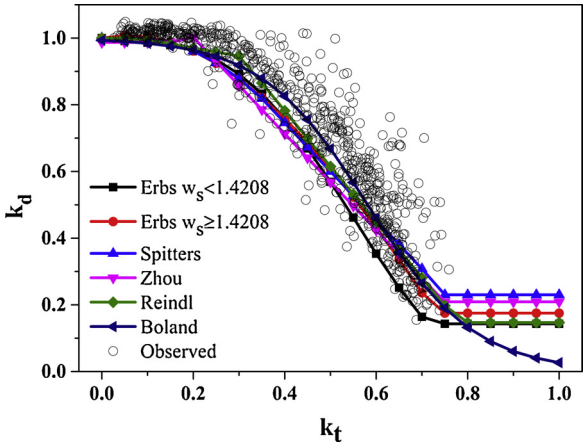


**Fig. 2.** Comparison of the diffuse fraction ($k_d$) models and comparison with the observed $k_d$. $k_t$, clearness index. $w_s$, sunset hour angle.

## 3. Results

### 3.1. Comparison of $k_d$ model performance

Comparison of calculation results for the five $k_d$ models are shown in Fig. 2. The calculated $k_d$ values for the five models were similar when $k_t$ was smaller than 0.25. The $k_d$ values estimated by the Boland model were greater than other models when $k_t$ ranged between 0.35 and 0.60. The differences among the calculated $k_d$ values were greatest when $k_t$ was larger than 0.75. However, our measured dataset only had one $k_t$ data point greater than 0.75. The relationship between observed $k_d$ and $k_t$ is also shown in Fig. 2. Observed $k_d$ values became more scattered as $k_t$ became greater than 0.25. For example, at $k_t$ = 0.5, the observed $k_d$ values ranged from 0.37 to 1.00 (Fig. 2). Simulated $k_d$ by these five models varied linearly with $k_t$. Therefore, future research should be directed towards improving the simulation accuracy of the model to identify the factors influencing $k_d$ variation under cloudy conditions.

The RE values (averaged by $k_t$ at intervals of 0.05) are shown in Fig. 3. Most of the RE values were positive, indicating that $k_d$ was underestimated by all five models for almost the entire range of $k_t$ values. This may be a result of more aerosols inducing an increase in $k_d$ at SX. The RE values of the five $k_d$ models were similar to each other and smaller when $k_t$ was less than 0.25. The RE values became greater and increased with increasing $k_t$ except at the 0.65–0.70 $k_t$ interval. The RE values of the Boland model were obviously smaller than those produced be the other models when $k_t$ ranged between 0.35 and 0.60.

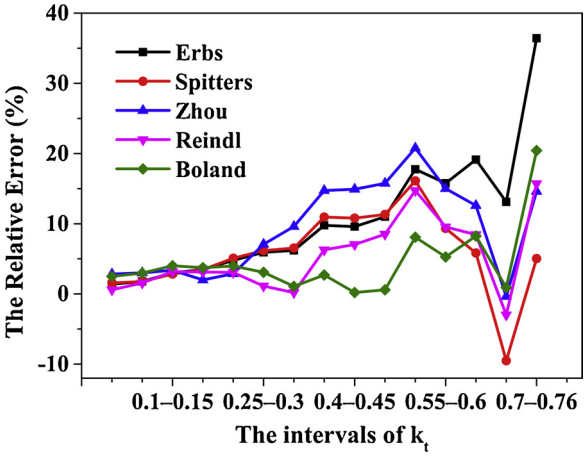


**Fig. 3.** Relative error (%) of five diffuse fraction models averaged by $k_t$ at an interval of 0.05.

**Table 6**
Comparison of five diffuse fraction models in terms of relative mean bias deviation (MBD, %) and root mean square deviation (RMSD).

| | MBD | RMSD |
|---|---|---|
| Erbs | 11.2 | 0.197 |
| Spitters | 6.1 | 0.181 |
| Zhou | 10.0 | 0.189 |
| Reindl | 5.7 | 0.171 |
| Boland | 4.3 | 0.162 |

Comparisons of the five models in terms of MBD and RMSD are shown in Table 6. The Boland model performed the best (as characterized by the minimum values of MBD and RMSD), followed by the Reindl and Spitters models. Therefore, the Boland model was chosen for modeling $k_d$ in this research.

### 3.2. Environmental conditions during research periods

Environmental conditions from jointing to milky maturity of winter wheat at YC and SX are shown in Table 3. Averaged over the 4-year periods, PAR and temperature were 28.6 mol $m^{-2}$ $d^{-1}$ and 17.3 ℃, respectively, at YC, with values of 30.9 mol $m^{-2}$ $d^{-1}$ and 15.4 ℃, respectively, at SX. VPD at YC was higher than at SX (except for 2011 at SX) during the measurement period and precipitation was less at YC than at SX. There was likely no water stress during the wheat growing season at YC due to flood irrigation, nor at SX due to adequate precipitation (except for 2011). Winter wheat at SX was likely subjected to some degree of water stress in 2011 due to lower precipitation and no irrigation. VPD from jointing to milky maturity of winter wheat at SX in 2011 was greater than during the other years at SX due to higher PAR and temperature and lower precipitation. The SWC during 2011 at SX was much lower than during the other years at this site.

### 3.3. Seasonal variation of GPP and LUE

The seasonal variation of GPP (Fig. 4a, b) at both locations increased first and then decreased. The GPP values for 2011 at SX (Fig. 4b) were obviously lower throughout the growing season than during the other three years because of water stress. The change of GPP from jointing to milky maturity, which was from early-mid April to mid-late May at YC and from mid-late March to early-mid May at SX, was relatively stable. Therefore, these periods when LAI was greater than or equal to 3 were chosen for analyzing the impact of environmental factors on GPP and LUE. GPP at YC ranged between 4.49 and 15.86 g C $m^{-2}$ $d^{-1}$, and at SX GPP ranged from 0.82 to 16.22 g C $m^{-2}$ $d^{-1}$ during these periods.

The trends of LUE (Fig. 4c, d) were similar to the changes of GPP. From jointing to milky maturity, LUE ranged between 0.190 and 0.655 g C $mol^{-1}$ at YC and between 0.083 and 0.622 g C $mol^{-1}$ at SX, with mean values of 0.379 and 0.304 g C $mol^{-1}$, respectively. Most of the LUE values at YC were greater than those at SX during the research periods.

### 3.4. Impacts of environmental factors on GPP and LUE

The total and direct effects of environmental factors (PAR, $k_d$, Ta, VPD, and SWC) on GPP and LUE at YC and SX are shown in Table 7. All of the direct effects of $k_d$ on GPP and LUE at both locations were positive, indicating that an increase in $k_d$ while maintaining all other variables fixed increased GPP and LUE.

All impact factors were significantly correlated with GPP at YC. PAR was the most highly correlated parameter with GPP. PAR had the greatest direct effect on GPP, followed by $k_d$. VPD had no significant direct effect on GPP. PAR, $k_d$, and VPD had significant total effects on LUE at YC, and $k_d$ was the most highly correlated parameter with LUE. All environmental factors had significant total effects on GPP at SX, with PAR having the greatest correlation coefficients. PAR had the greatest direct effect on GPP, with the value being 1.528. Standardized partial regression coefficients (direct effect values) may exceed the bounds of (-1, 1) if there were two or more independent variables that were correlated (Deegan, 1978). PAR and $k_d$ had the greatest correlation coefficients with LUE, followed by VPD. The direct effect of $k_d$ on LUE was the greatest among all influencing factors, but the direct effect

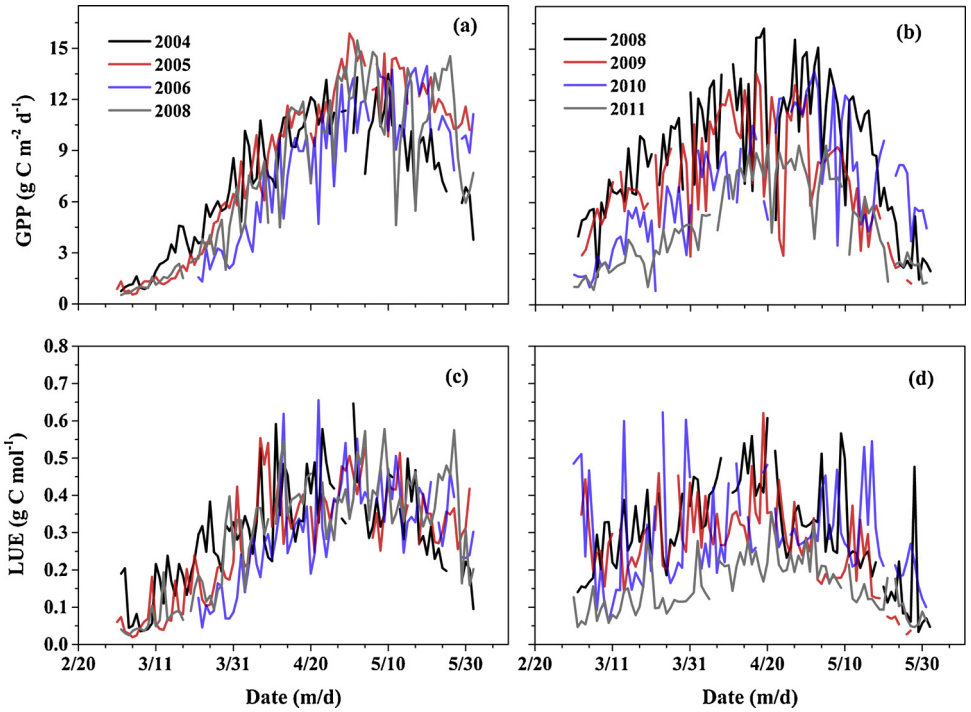


**Fig. 4.** Gross primary production (GPP) and light use efficiency (LUE) during wheat rapid growth stage from1 March to 31 May at Yucheng (a, c) and Shouxian (b, d), China.

**Table 7**
The total (correlation coefficients) and direct effects of environmental factors on gross primary production (GPP) and light use efficiency (LUE) at Yucheng (YC) and Shouxian (SX), China.

| Station | | PAR | $k_d$ | Ta | VPD | SWC |
|---|---|---|---|---|---|---|
| YC | Total effect on GPP | 0.546** | −0.364** | 0.432** | 0.352** | 0.225** |
| | Direct effect on GPP | 0.828** | 0.322 | 0.295** | −0.127 | 0.129* |
| | Total effect on LUE | −0.707** | 0.742** | 0.064 | −0.396** | 0.037 |
| | Direct effect on LUE | −0.483** | 0.262 | 0.223** | −0.084 | 0.089 |
| SX | Total effect on GPP | 0.570** | −0.393** | 0.312** | 0.222* | 0.371** |
| | Direct effect on GPP | 1.528** | 0.835** | 0.154* | −0.261** | 0.382** |
| | Total effect on LUE | −0.634** | 0.699** | −0.067 | −0.554** | 0.517** |
| | Direct effect on LUE | −0.144 | 0.416** | 0.285** | −0.206 | 0.398** |

PAR, photosynthetically active radiation; $k_d$, diffuse radiation fraction; Ta, air temperature; VPD, vapor pressure deficit; SWC, soil water content.
** Significant $P < 0.01$.
* Significant $P < 0.05$.

of PAR on LUE was not significant. The total and direct effect of SWC on GPP and LUE were all significant, probably because winter wheat growth was limited by SWC in the dry year (2011) at SX. In conclusion, PAR and $k_d$ were the most important parameters influencing GPP and LUE respectively.

The indirect effects describe how $k_d$ influenced GPP and LUE through other variables (Table 8). $k_d$ mainly interacted with PAR to impact GPP and LUE. The indirect effects of $k_d$ through other variables were all small as indicated by the small correlation coefficients between $k_d$ and other variables or small direct effects of other variables on GPP and LUE.

### 3.5. Relationships between $k_d$ and LUE

The positive relationships between $k_d$ and LUE for winter wheat were both significantly linear (Fig. 5, $P < 0.001$), with slopes of 0.331 and 0.321 g C $mol^{-1}$ at YC and SX, respectively. The similar slopes at these two stations indicated that the differences in growth environments had little effect on the relationship between $k_d$ and LUE. Differences in $k_d$ accounted for 55 and 49% of the variation in LUE between winter wheat jointing and milky maturity at YC and SX, respectively. LUE values in 2011 at SX were consistently lower than those during the other three years (Fig. 4d), resulting in greater scatter of the data at SX.

The trends of simulated LUE by APSIM-Nwheat and observed LUE with $k_d$ are shown in Fig. 6. In this figure, we focus on the trend and not on magnitude of the simulated and observed LUE values, as simulated LUE by APSIM-Nwheat are potential. Simulated LUE increased by 23% when $k_d$ increased from 0.24 to 0.80 at YC, while observed LUE increased by 70%, which was estimated by fitting equation in Fig. 5 ($y = 0.331 x + 0.185$). Similar trend was found at SX, where simulated LUE increased by 18% and observed LUE increased by 121% (estimating by $y = 0.321 x + 0.097$) when $k_d$ increased from 0.20 to 0.80. The increased rate of simulated LUE was greater than observed one when $k_d$ was greater than 0.80. These results showed that the LUE module in APSIM-Nwheat underestimated the increase rate of LUE when sky types changed from sunny to cloudy ($0.2 \le k_d \le 0.8$). And the module overestimated the increase rate of LUE on overcast days ($0.8 < k_d \le 1.0$). Therefore, the LUE module in APSIM-Nwheat should be improved. The effect of $k_d$ on LUE should be added to the module to improve the simulation accuracy.

**Table 8**
The indirect effects from diffuse radiation fraction ($k_d$) through other environmental factors to gross primary production (GPP) and light use efficiency (LUE) at Yucheng (YC) and Shouxian (SX), China.

| Station | Indirect effects from $k_d$ via: | PAR | Ta | VPD | SWC |
|---|---|---|---|---|---|
| YC | GPP | −0.750 | 0 | 0.068 | −0.005 |
| | LUE | 0.438 | 0 | 0.045 | −0.003 |
| SX | GPP | −1.423 | −0.023 | 0.159 | 0.062 |
| | LUE | 0.134 | −0.042 | 0.125 | 0.064 |

PAR, photosynthetically active radiation; Ta, air temperature; VPD, vapor pressure deficit; SWC, soil water content.

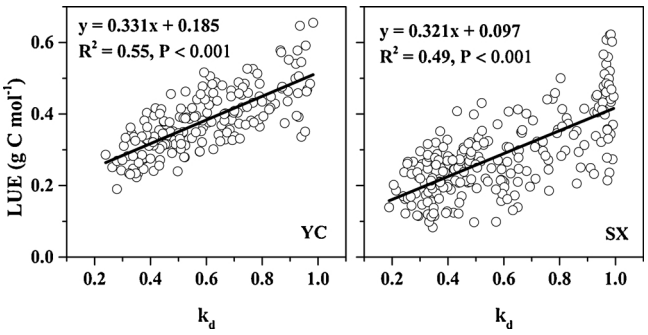


**Fig. 5.** Relationship between diffuse radiation fraction ($k_d$) and light use efficiency (LUE) from jointing to milky maturity of winter wheat at Yucheng (YC) and at Shouxian (SX).

### 3.6. Relationships between $k_d$ and GPP

The relationships between $k_d$ and GPP from jointing to milky maturity of winter wheat at YC and SX are shown in Fig. 7. GPP initially increased and then decreased with increasing $k_d$. Quadratic polynomials were therefore used to fit relationships between these two parameters. The coefficients of determination were 0.35 and 0.24 at YC and SX, respectively. There was more scatter in the relationship between $k_d$ and GPP at SX than at YC, because GPP during 2011 was consistently lower than in the other three years due to water stress during the wheat growing season (Fig. 4). The $k_d$ values at which maximum GPP occurred were determined to be 0.55 and 0.50 at YC and SX respectively. Therefore, the sky conditions in which $k_d$ was 0.55 and 0.50 were the most favorable for carbon assimilation of winter wheat at YC and SX, respectively.

## 4. Discussion

### 4.1. Modelling $k_d$ in the North China Plain

Accurate estimates of $k_d$ through modeling would determine whether the impact of $k_d$ on LUE and GPP could be correctly evaluated (Lee et al., 2018) in the North China Plain, as there are many stations having no observations of diffuse radiation. All five of the $k_d$ models tended to underestimate $k_d$ for all $k_t$ intervals. We found the Boland model to be the best of the five $k_d$ models for predicting diffuse fraction for our two-year validation dataset. These results were different from previous

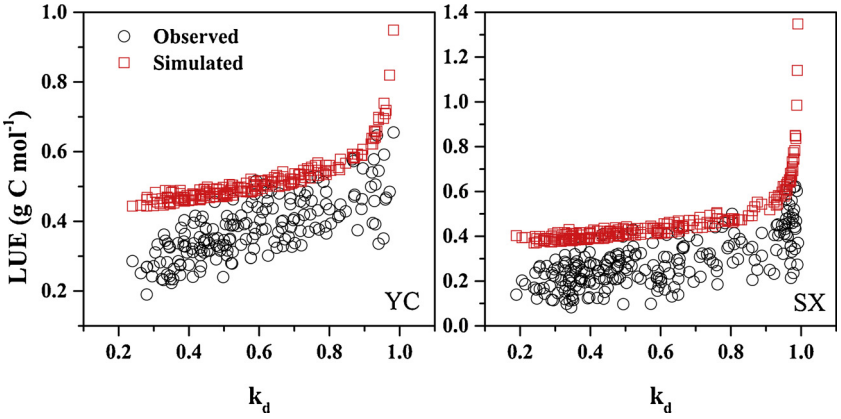


**Fig. 6.** Trend of simulated light use efficiency (LUE) by APSIM-Nwheat with diffuse radiation fraction ($k_d$) and variation of observed LUE with $k_d$ at Yucheng (YC) and Shouxian (SX).

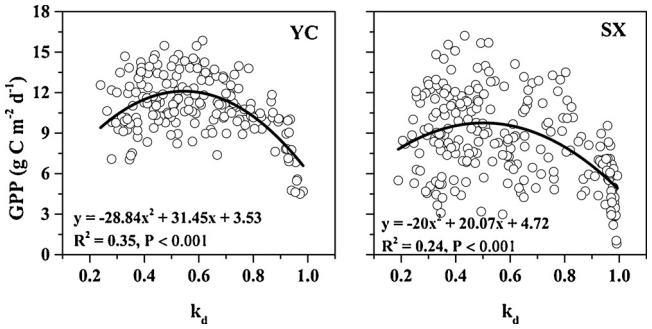


**Fig. 7.** Relationship between diffuse radiation fraction ($k_d$) and gross primary production (GPP) from jointing to milky maturity of winter wheat at Yucheng (YC) and at Shouxian (SX).

comparison studies (Dervishi and Mahdavi, 2012; Kuo et al., 2014), probably because the spatial variability of the relationship between $k_d$ and $k_t$ (Boland et al., 2001; Oliveira et al., 2002). Observed $k_d$ values were scattered and variably under cloudy conditions (Fig. 2). The factors causing changes in $k_d$ should be determined in order to improve $k_d$ model accuracy. Perhaps the amount and type of cloud cover and aerosols in the atmosphere, and how these influences diffuse radiation should be considered in $k_d$ models.

### 4.2. Quantitative relationship between $k_d$ and LUE of winter wheat

Accurate simulation modeling of winter wheat requires correct quantification of the relationship between $k_d$ and LUE as LUE is an important parameter for simulating potential biomass production with crop models. Previous modeling studies have assumed crop LUE to be a constant or stage-dependent parameter (Chen et al., 2010), or that daily LUE could be simulated using daily solar radiation (Yang et al., 2013). The simulated potential wheat yields significantly decreased from 1961 to 2003 at Beijing due to declining solar radiation when using APSIM model version 5.3, which employs a constant for LUE (Chen et al., 2010). However, our simulated results showed that wheat yield had no significant trend during the past 48 years at Beijing when using APSIM-Nwheat, which calculates daily LUE using daily solar radiation (Yang et al., 2013). The difference of simulation results is mainly due to the different LUE modules in the two versions of APSIM model. Through path and regression analysis of winter wheat field observations, we found that $k_d$ was the most important factor influencing winter wheat LUE in the North China Plain, with $k_d$ explaining about 52% of the variation in LUE. Huang et al. (2014) reported that variation in the cloudiness index (CI, 1 – incident PAR/potential incident PAR) explained 74 to 85% of the LUE for forest ecosystems, but only 24 to 50% of the variability of LUE for grassland ecosystems. Alton et al. (2007) reported that the magnitude of the influence of $k_d$ on LUE was affected by LAI of different vegetative canopies. Overall, $k_d$ should be considered an important parameter for correctly estimating LUE in crop models.

The effect of $k_d$ on LUE were not sufficient considered in the LUE module of APSIM-Nwheat, although simulated LUE increased with increasing $k_d$. The LUE module underestimated the increase rate of LUE when $k_d$ increased from 0.20 to 0.80 (Fig. 6). The impact of $k_d$ on LUE should be added in crop models. Previous studies also have added quantitative relationships between $k_d$ and LUE to crop models. For example, Greenwald et al. (2006) added a cubic equation in CERES to define the relationship between the increase of LUE and daily $k_d$ to estimate the influence of aerosols on crop yield. Chen et al. (2010) added a linear equation between LUE and $k_d$ in APSIM (version 5.3) which assumed LUE of wheat increased linearly to 100% when $k_d$ changed from 0 to 1.0 in order to quantify climate change effects on crop growth in the North China Plain. The relationship equations between $k_d$ and LUE were important for the modeling results. Therefore, it is important to accurately define the quantitative relationship between $k_d$ and LUE based on local field observations.

Consistent with previous studies (Choudhury, 2000; Roderick et al., 2001; Rodriguez and Sadras, 2007), we found a significant linear relationship between $k_d$ and LUE of winter wheat in the North China Plain (slope of about 0.326 g C $mol^{-1}$). Choudhury (2000), using both modeled and measured wheat data, reported slopes for $k_d$ versus LUE of 0.031 and 0.043 mol $mol^{-1}$ for LAI values of 0.5 and 5.2, respectively. Simulated results for wheat (for the period between 20 days before and 14 days after anthesis) showed that LUE (g $MJ^{-1}$) = 1.6 × $k_d$ + 1.5 (Rodriguez and Sadras, 2007). The comparison of slopes from these previous studies is difficult due to the different units used to report LUE. The various units were derived from several different definitions of LUE, thereby influencing the results and interpretation of the LUE model (Gitelson and Gamon, 2015). The quantitative relationship between $k_d$ and LUE likely needs to be validated with more observed data at various locations and environments.

### 4.3. Comprehensive effects of $k_d$ and PAR on GPP of winter wheat

There is no consensus about the effect of $k_d$ on GPP because GPP variation is influenced by various environmental factors and ecosystem types (Zhang et al., 2011; Cheng et al., 2015). Many studies have reported that GPP of forest canopies increased when there was more diffuse sky radiation (Gu et al., 1999; Oliphant et al., 2011; Urban et al., 2012; Zhang et al., 2011). However, simulation studies reported that carbon uptake did not significantly increase on cloudy days as compared with clear days because of reductions in total solar radiation

(Alton, 2008; Alton et al., 2007). Our path analysis found that GPP of winter wheat would increase with increasing $k_d$ while maintaining all other variables fixed. Quadratic relationships were also found between $k_d$ and GPP in our study, which showed that GPP initially increased and then decreased with increasing $k_d$. Values of $k_d$ explained up to 35% of the variation of GPP for winter wheat, similar to the results of Cheng et al. (2015) who found that $k_d$ explained up to 41% of seasonal variations in GPP in croplands. There were optimal $k_d$ values for maximum GPP at YC and SX (0.55 and 0.50, respectively). There may be some changes in these results if there was nutrients or water stress during wheat growth, as GPP is vulnerable to environmental factors. Others have reported that cloudy days with moderate solar radiation were more favorable for carbon uptake of forest, grassland, and shrub ecosystems (Gu et al., 2002; Min and Wang, 2008; Zhang et al., 2011).

## 5. Conclusions

The effects of environmental factors (especially $k_d$) on LUE and GPP of winter wheat were evaluated using an eddy covariance data set (eight site-years) from two winter wheat locations in the North China Plain. This research identified $k_d$ as the main factor influencing LUE variation. About 52% of the variation in LUE was explained by variation in $k_d$. Therefore, $k_d$ should be the main factor to consider in the simulation of LUE for winter wheat. The relationship between $k_d$ and LUE was significantly linear with a slope of about 0.326 g C $mol^{-1}$. GPP initially increased and then decreased with increasing $k_d$. Cloudy days (where $k_d$ was about 0.53) resulted in maximum GPP for winter wheat in the North China Plain. Of five models evaluated for estimating $k_d$, the Boland model was best for modeling of $k_d$ based on $k_t$ in the North China Plain. This is an important finding due to the lack of measured diffuse radiation data across the North China Plain and the importance of having correct values of $k_d$ to accurately model LUE and GPP in this major wheat production region. All of the results were important for accurate modeling of winter wheat production for this area and predicting and planning for the effects of future climate change.

## Acknowledgments

This work was supported by the National Natural Science Foundation of China (Grant no. 41730645 and 31400416) and by the Natural Science Foundation of Jiangsu Province (Grant no. BK20140988).

## References

Allen, R.G., Pereira, L.S., Raes, D., et al., 2006. FAO Irrigation and Drainage Paper No. 56. Crop Evapotranspiration[M] (guidelines for Computing Crop Water Requirements). pp. 46.
Alton, P.B., 2008. Reduced carbon sequestration in terrestrial ecosystems under overcast skies compared to clear skies. Agric. For. Meteorol. 148, 1641–1653.
Alton, P.B., North, P.R., Los, S.O., 2007. The impact of diffuse sunlight on canopy light-use efficiency, gross photosynthetic product and net ecosystem exchange in three forest biomes. Glob. Change Biol. Bioenergy 13 (4), 776–787.
Asseng, S., Keating, B., Fillery, I., et al., 1998. Performance of the APSIM-wheat model in Western Australia. Field Crops Res. 57, 163–179.
Boland, J., Scott, L., Luther, M., 2001. Modelling the diffuse fraction of global solar radiation on a horizontal surface. Environmetrics 12, 103–116.
Boland, J., Ridley, B., Brown, B., 2008. Models of diffuse solar radiation. Renew. Energy 33, 575–584.
Chen, C., Wang, E.L., Yu, Q., et al., 2010. Quantifying the effects of climate trends in the past 43 years (1961–2003) on crop growth and water demand in the North China Plain. Clim. Change 100, 559–578.
Cheng, S.J., Bohrer, G., Steiner, A.L., et al., 2015. Variations in the influence of diffuse light on gross primary productivity in temperate ecosystems. Agric. For. Meteorol. 201, 98–110.
Choudhury, B.J., 2000. A sensitivity analysis of the radiation use efficiency for gross photosynthesis and net carbon accumulation by wheat. Agric. For. Meteorol. 101, 217–234.
Choudhury, B.J., 2001. Modeling radiation- and carbon-use efficiencies of maize, sorghum, and rice. Agric. For. Meteorol. 106, 317–330.
Cruse, M.J., Kucharik, C.J., Norman, J.M., 2015. Using a simple apparatus to measure direct and diffuse photosynthetically active radiation at remote locations. PLoS One 10.
Deegan, J., 1978. On the occurrence of standardized regression coefficients greater than one. Educ. Psychol. Meas. 38 (4), 873–888.
Dengel, S., Grace, J., 2010. Carbon dioxide exchange and canopy conductance of two coniferous forests under various sky conditions. Oecologia 164 (3), 797–808.
Dervishi, S., Mahdavi, A., 2012. Computing diffuse fraction of global horizontal solar radiation: a model comparison. Sol. Energy 86, 1796–1802.
Dunn, A.L., Barford, C.C., Wofsy, S.C., et al., 2007. A long-term record of carbon exchange in a boreal black spruce forest: means, responses to interannual variability, and decadal trends. Glob. Change Biol. Bioenergy 13, 577–590.
Erbs, D.G., Klein, S.A., Duffie, J.A., 1982. Estimation of the diffuse radiation fraction for hourly, daily and monthly-average global radiation. Sol. Energy 28 (4), 293–302.
Falge, E., Baldocchi, D., Olson, R., et al., 2001. Gap filling strategies for defensible annual sums of net ecosystem exchange. Agric. For. Meteorol. 107, 43–69.
Gitelson, A.A., Gamon, J.A., 2015. The need for a common basis for defining light-use efficiency: implications for productivity estimation. Remot. Sens. Environ. 156, 196–201.
Greenwald, R., Bergin, M.H., Jin, X., et al., 2006. The influence of aerosols on crop production: a study using the CERES crop model. Agric. Syst. 89, 390–413.
Gu, L.H., Fuentes, J.D., Shugart, H.H., et al., 1999. Responses of net ecosystem exchanges of carbon dioxide to changes in cloudiness results from two North American deciduous forests. J. Geophys. Res. Atmos. 104 (D24), 31421–31434.
Gu, L.H., Baldocchi, D., Verma, S.B., et al., 2002. Advantages of diffuse radiation for terrestrial ecosystem productivity. J. Geophys. Res. Atmos. 107 (D6), 4050.
Gu, L.H., Baldocchi, D.D., Wofsy, S.C., et al., 2003. Response of a deciduous forest to the Mount Pinatubo eruption: enhanced photosynthesis. Science 299, 2035–2038.
Huang, K., Wang, S.Q., Zhou, L., et al., 2014. Impacts of diffuse radiation on light use efficiency across terrestrial ecosystems based on eddy covariance observation in China. PLoS One 9 (11), e110988. https://doi.org/10.1371/journal.pone.0110988.
Huxman, T.E., Turnipseed, A.A., Sparks, J.P., et al., 2003. Temperature as a control over ecosystem CO2 fluxes in a high-elevation, subalpine forest. Oecologia 134 (4), 537–546.
Jing, X., Huang, J., Wang, G., et al., 2010. The effects of clouds and aerosols on net ecosystem $CO_2$ exchange over semi-arid loess plateau of northwest China. Atmos. Chem. Phys. 10, 8205–8218.
Kanniah, K.D., Beringer, J., Hutley, L., 2013. Exploring the link between clouds, radiation, and canopy productivity of tropical savannas. Agric. For. Meteorol. 182–183 (12), 304–313.
Kanniah, K.D., Beringer, J., North, P., et al., 2012. Control of atmospheric particles on diffuse radiation and terrestrial plant productivity: a review. Prog. Phys. Geogr. 36 (2), 209–237.
Keating, B.A., Meinke, H., Probert, M.E., et al., 2001. NWheat: documentation and performance of a wheat module for APSIM. Trop. Agric. Tech. Memo.
Kuo, C., Chang, W., Chang, K., 2014. Modeling the hourly solar diffuse fraction in Taiwan. Renew. Energy 66, 56–61.
Lee, M.S., Hollinger, D.Y., Keenan, T.F., et al., 2018. Model-based analysis of the impact of diffuse radiation on $CO_2$ exchange in a temperate deciduous forest. Agric. For. Meteorol. 249, 377–389.
Li, J., Yu, Q., Sun, X.M., et al., 2006. Carbon dioxide exchange and the mechanism of environmental control in a farmland ecosystem in North China Plains. Sci. China Ser. D Earth Sci. 49 (S2), 226–240.
Liu, B.Y.H., Jordan, R.C., 1960. The interrelationship and characteristic distribution of direct, diffuse and total solar radiation. Sol. Energy 4 (3), 1–19.
Lloyd, J., Taylor, J.A., 1994. On the temperature dependence of soil respiration. Funct. Ecol. 8, 315–323.
McMillen, R.T., 1988. An eddy correlation technique with extended applicability to non-simple terrain. Boundary. Meteorol. 43, 231–245.
Min, Q., Wang, S., 2008. Clouds modulate terrestrial carbon uptake in a midlatitude hardwood forest. Geophys. Res. Lett. 35 (2), L02406.
Oliphant, A.J., Dragoni, D., Deng, B., et al., 2011. The role of sky conditions on gross primary production in a mixed deciduous forest. Agric. For. Meteorol. 115, 781–791.
Oliveira, A.P., Escobedo, J.F., Machado, A.J., Soares, J., 2002. Correlation models of diffuse solar-radiation applied to the city of São Paulo, Brazil. Appl. Energy 71, 59–73.
Reindl, D.T., Beckman, W.A., Duffie, J.A., 1990. Diffuse fraction correlations. Sol. Energy 45, 1–7.
Ren, X.L., He, H.L., Zhang, L., et al., 2013. Spatiotemporal variability analysis of diffuse radiation in China during 1981–2010. Ann. Geophys. Discuss. 31, 277–289.
Ritchie, J., Godwin, D., Otter-Nacke, S., 1985. CERES-Wheat: A User-oriented Wheat Yield Model. Preliminary Documentation. AGRISTARS Publication No. YM-U3-04442-JSC-18892. Michigan State University, East Lansing, USA.
Roderick, M.L., Farquhar, G.D., Berry, S.L., et al., 2001. On the direct effect of clouds and atmospheric particles on the productivity and structure of vegetation. Oecologia 129, 21–30.
Rodriguez, D., Sadras, V., 2007. The limit to wheat water-use efficiency in eastern Australia I: gradients in the radiation environment and atmospheric demand. Aust. J. Agric. Res. 58, 287–302.
Schiermeier, Q., 2006. Oceans cool off in hottest years. Nature 442, 854–855.
Spiertz, J.H.J., Van de Haar, H., 1978. Differences in grain growth, crop photosynthesis and distribution of assimilates between a semi-dwarf and a standard cultivar of winter wheat. Neth. J. Agric. Sci. 26, 233–249.
Spitters, C.J.T., Toussaint, H.A.J.M., Goudriaan, J., 1986. Separating the diffuse and direct component of global radiation and its implications for modeling canopy photosynthesis Part I. Components of incoming radiation. Agric. For. Meteorol. 38, 217–229.
Tong, X., Li, J., Nolan, R.H., Yu, Q., 2017. Biophysical controls of soil respiration in a

wheat-maize rotation system in the North China Plain. Agric. For. Meteorol. 246, 231–240.
Urban, O., Klem, K., Ač, A., Havránková, K., et al., 2012. Impact of clear and cloudy sky conditions on the vertical distribution of photosynthetic $CO_2$ uptake within a spruce canopy. Funct. Ecol. 26 (1), 46–55.
Wang, S., Huang, K., Yan, H., et al., 2015. Improving the light use efficiency model for simulating terrestrial vegetation gross primary production by the inclusion of diffuse radiation across ecosystems in China. Ecol. Complex 23, 1–13.
Wang, S., Ibrom, A., Bauer-Gottwein, P., et al., 2018. Incorporating diffuse radiation into a light use efficiency and evapotranspiration model: an 11-year study in a high latitude deciduous forest. Agric. For. Meteorol. 248, 479–493.
Watanabe, I., 1975. Transformation factor from carbon dioxide net assimilation to dry weight in crops. III. Rice. Proc. Crop Sci. Soc. Jpn. 44, 409–413.
Webb, E.K., Pearman, G.I., Leuning, R., et al., 1980. Correction of flux measurements for density effects due to heat and water vapor transfer. Q. J. R. Meteorol. Soc. 106, 85–100.
Williams, I.N., Riley, W.J., Kueppers, L.M., et al., 2016. Separating the effects of phenology and diffuse radiation on gross primary productivity in winter wheat. J. Geophys. Res. Biogeosci. 121 (7), 1903–1915.
Wu, J., Albert, L.P., Lopes, A.P., et al., 2016. Leaf development and demography explain photosynthetic seasonality in Amazon evergreen forests. Science 351 (6276), 972–976.
Yang, X., Zhao, C., Guo, J., et al., 2016. Intensification of aerosol pollution associated with its feedback with surface solar radiation and winds in Beijing. J. Geophys. Res. Atmos. 121, 4093–4099.
Yang, X.Y., Asseng, S., Wong, M.T.F., et al., 2013. Quantifying the interactive impacts of global dimming and warming on wheat yield and water use in China. Agric. For. Meteorol. 182–183, 342–351.
Yang, X.Y., McMaster, G.S., Yu, Q., 2018. Spatial patterns of relationship between wheat yield and yield components in China. Int. J. Plant Prod. 12, 61–71.
Yu, G.R., Zhang, L.M., Sun, X.M., et al., 2008. Environmental controls over carbon exchange of three forest ecosystems in eastern China. Glob. Change Biol. Bioenergy 14, 2555–2571.
Yuan, W., Cai, W., Xia, J., et al., 2014. Global comparison of light use efficiency models for simulating terrestrial vegetation gross primary production based on the LaThuile database. Agric. For. Meteorol. 192, 108–120.
Zhang, M., Yu, G.R., Zhuang, J., et al., 2011. Effects of cloudiness change on net ecosystem exchange, light use efficiency, and water use efficiency in typical ecosystems of China. Agric. For. Meteorol. 151 (7), 803–816.
Zhu, Z.L., Sun, X.M., Wen, X.F., et al., 2006. Study on the processing method of nighttime $CO_2$ eddy covariance flux data in ChinaFLUX. Sci. China Ser. D: Earth Sci. 49 (Supp. II), 36–46.